

Aged garlic extract major constituent S-1-propenyl-l-cysteine inhibits proinflammatory mRNA expression in bronchial epithelial IB3-1 cells exposed to the BNT162b2 vaccine

CHIARA PAPI¹, JESSICA GASPARELLO¹, GIOVANNI MARZARO², ALBERTO MACONE³,
MATTEO ZURLO¹, FEDERICA DI PADUA¹, PASQUALE FINO⁴,
ENZO AGOSTINELLI^{4,5}, ROBERTO GAMBARI¹ and ALESSIA FINOTTI¹

¹Department of Life Sciences and Biotechnology, Ferrara University, I-44121 Ferrara, Italy; ²Department of Diagnostics and Public Health, University of Verona, I-37134 Verona, Italy; ³Department of Biochemical Sciences 'A. Rossi Fanelli', Sapienza University of Rome, I-00185 Rome, Italy; ⁴Department of Sensory Organs, Sapienza University of Rome, Policlinico Umberto I, I-00161 Rome, Italy; ⁵International Polyamines Foundation 'ETS-ONLUS', I-00159 Rome, Italy

Received October 7, 2024; Accepted April 15, 2025

DOI: 10.3892/etm.2025.12903

Abstract. A simple experimental model system was developed and validated for the identification and characterization of molecules exhibiting the ability to inhibit the expression of genes activated during the coronavirus disease 2019 (COVID-19) 'cytokine storm' for the present study. Biomolecules derived from herbal medicinal extracts have been proposed as anti-inflammatory strategies for reducing COVID-19 'cytokine storm' and the associated Acute Respiratory Distress Syndrome. Considering this, the present study focused on a major component of Aged Garlic Extract (AGE), S-1-propenylcysteine (S1PC). The human bronchial epithelial IB3-1 cell line was used to upregulate the expression of proinflammatory genes after exposure to the COVID-19 BNT162b2 vaccine. The effects of S1PC were then studied following continuous treatment for 2 days in BNT162b2-exposed IB3-1 cells. The concentrations of S1PC were 1, 5, 10, 25, 50 and 100 μ M. GC-MS analysis was performed in order to characterize the S1PC used in the experiments. Reverse-transcription-quantitative PCR and western blotting analysis revealed the accumulation of

Spike mRNA and protein in BNT162b2-exposed IB3-1 cells. Subsequently, the effects of S1PC on the several biological and biochemical parameters were analyzed, including cell viability, apoptosis, the NF- κ B pathway and the expression of proinflammatory factors. Molecular docking analysis was performed to obtain preliminary information on the putative mechanism(s) of action of S1PC. The results of the present study demonstrate that exposure of epithelial IB3-1 cells to the COVID-19 BNT162b2 vaccine is associated with a sharp increase in the expression of the transcription factor NF- κ B and NF- κ B-regulated genes, including *IL-6*, *IL-8* and granulocyte-colony stimulation factor 9 (G-CSF). Treatment with S-1-propenyl-l-cysteine (S1PC) was found to reverse the BNT162b2-induced upregulation of NF- κ B, *IL-6*, *IL-8* and G-CSF. These effects were not associated with inhibition of cell viability, induction of apoptosis or a decrease of the cell growth rate, as demonstrated by the results based on the analysis of cell number and the proportion of early and late apoptotic cells within the cell population. With respect to possible mechanisms of action, molecular docking and molecular dynamics simulations strongly suggest that S1PC interacts with Toll-like receptor-4, possibly explaining the inhibitory effects on NF- κ B and NF- κ B-regulated genes. Therefore, S1PC should be further evaluated as a potential inhibitor of this COVID-19 'cytokine storm'. However, further experimental studies are needed to identify other agents that can also able to inhibit gene expression induced by the COVID-19 BNT162b2 vaccine and to verify whether combined treatments with S1PC could be proposed to obtain even superior inhibitory effects.

Correspondence to: Professor Alessia Finotti or Professor Roberto Gambari, Department of Life Sciences and Biotechnology, Ferrara University, Via Fossato di Mortara 74, I-44121 Ferrara, Italy
E-mail: alessia.finotti@unife.it
E-mail: gam@unife.it

Abbreviations: ARDS, acute respiratory distress syndrome; COVID-19, coronavirus disease 2019; RT-qPCR, reverse transcription-quantitative PCR; SARS-CoV-2, Severe Acute Respiratory Syndrome Coronavirus 2

Keywords: S-1-propenyl-l-cysteine, aged garlic extract, inflammation, anti-severe acute respiratory syndrome coronavirus 2, BNT162b2 vaccine, spike, IB3-1 cells

Introduction

The coronavirus disease 2019 (COVID-19) pandemic is characterized by high-level infection by severe acute respiratory syndrome coronavirus 2 (SARS-CoV-2). The most severe of its symptoms is caused by a hyperinflammatory condition due to the excessive production of cytokines and chemokines, known as 'cytokine storm' (1,2). COVID-19 cytokine storm primarily

originates from T cells, macrophages, monocytes, dendritic cells and endothelial cells (3-5), where it is induced by a molecular interaction between the SARS-CoV-2 S-protein and angiotensin-converting enzyme 2 (ACE2). This is followed by complex intracellular changes that include hyperactivation of the transcription factor NF- κ B by the IL-6/STATs axis (6). These cellular changes are eventually associated with the life-threatening acute respiratory distress syndrome (ARDS), which mainly affects the lung and is a typical feature of patients with COVID-19 (7) exhibiting a severe form of the pathology (8,9). Accordingly, pharmacological anti-inflammatory strategies for anti-SARS-CoV-2 treatment based on targeting of IL-6 and IL-8 are highly impactful (10,11). Despite these important developments, further novel pharmacological approaches for treating hyperinflammatory ARDS are required, because different patients with COVID-19 can respond differently to the available treatments (12).

In this respect, various biomolecules derived from herbal medicinal extracts have been proposed for anti-inflammatory strategies to reduce COVID-19 'cytokine storm' and associated ARDS (13,14). Among the herbal medicinal extracts hypothesized to confer anti-inflammatory activities, aged garlic extract (AGE) is of particular interest (15). The preparation of AGE is performed by the immersion (which can be performed at room temperature) of fresh garlic in an aqueous ethanol solution over a prolonged period (≤ 20 months) (16). Experimental evidence exists demonstrating that this natural product possesses immunomodulatory and anticancer properties (15,16). Among the bioactive compounds that can be isolated from AGE, S-1-propenyl-L-cysteine (SIPC) has previously been studied, where it has been found to retain *in vitro* and *in vivo* biological (including anti-inflammatory) activities of interest in biomedicine (17-20).

The main aim of the present study was to assess the effects of SIPC on the expression of genes involved in the COVID-19 'cytokine storm'. The effects were studied using an experimental *in vitro* model system based on the human bronchial epithelial cell line IB3-1 (21) exposed to the COVID-19 BNT162b2 vaccine, according to previously validated protocols (22). After exposure to the BNT162b2 vaccine, the cells were cultured for 48 h in the presence of increasing concentrations of SIPC, before they were harvested for reverse transcription-quantitative PCR (RT-qPCR) analysis.

Materials and methods

Materials. All chemicals and reagents were analytical grade. SIPCTM (S-1-propenyl-L-cysteine) were obtained from Wakunaga Pharmaceutical Co., Ltd., Japan. SARS-COV-2 Spike recombinant glycoprotein (cat. no. ab49046) was purchased by Abcam. The purity was >90% as determined by SDS-PAGE.

Gas chromatography (GC)-mass spectrometry (MS) analysis. SIPC was analyzed by GC-MS as TBDMS derivatives according to Jiménez-Martín *et al.* (23).

SIPC was dissolved in 0.1 N HCl to a final concentration of 4 mg/ml. In total, 5 μ l these solutions were spiked with 10 μ l internal standard (3,4-dimethoxybenzoic acid, 0.1 mg/ml) and dried under N₂. Subsequently, 30 μ l pure

N-tert-butyldimethylsilyl-N-methyltrifluoroacetamide, followed by 30 μ l pyridine, was added. The mixture was then heated at 80°C for 1 h. The sample was neutralized afterwards with sodium bicarbonate and subjected to GC-MS analysis. The same derivatization protocol was used for the AGE powder (4 mg/ml 0.1 M HCl).

For all GC-MS analyses, an Agilent 7890B gas chromatograph coupled to a 5977B quadrupole mass selective detector (Agilent Technologies, Inc.) was employed. For chromatographic separations, an Agilent HP5ms fused-silica capillary column (30 m x 0.25 mm i.d.) (Agilent Technologies, Inc.) was used, coated with 5%-phenyl-95%-dimethylpolysiloxane (film thickness, 0.25 μ m) as stationary phase. Splitless injection was performed at 280°C. The column temperature program was set to 70°C (1 min), then to 300°C at a rate of 20°C/min and held for 10 min. The carrier gas was helium at a constant flow of 1.0 ml/min. The spectra were obtained in the electron impact mode at 70 eV ionization energy, ion source of 280°C and ion source vacuum of 10⁻⁵ Torr. MS analysis was performed simultaneously in total ion current (mass range scan in the range of m/z 50-600 at a rate of 0.42 scans per sec) and selected ion chromatogram mode. GC-SIM-MS analysis was performed by selecting the following ions: m/z 332 for SIPC and m/z 239 for 3,4-dimethoxybenzoic acid (internal standard).

Cell culture conditions and treatment with the BNT162b2 vaccine. The human bronchial epithelial IB3-1 cell line (Thermo Fischer Scientific, Inc.) (21) was cultured in LHC-8 medium (Gibco; Thermo Fischer Scientific, Inc.), supplemented with 5% FBS (Biowest) without antibiotics at a temperature of 37°C and 5% CO₂ (21). The BNT162b2 vaccine (COMIRNATYTM; lot. No. FP8191) was obtained from the Hospital Pharmacy of the University of Padova. The SIPC powder was freshly dissolved in culture medium, normally up to 50 mM, before each experiment. The solution was kept in the dark and used only once (15). For treatment with the BNT162b2 vaccine, IB3-1 cells were seeded at 200,000 cells/ml concentration. After 24 h at 37°C, 0.5 μ g/ml vaccine (22) was added just before the indicated concentrations of SIPC were added for an additional 48 h at 37°C of treatment, for determining the effects on SIPC on BNT162b2-induced gene expression. Following incubation, cells were detached from the plate by trypsinization, counted using a Beckman Coulter[®] Z2 cell counter (Beckman Coulter, Inc.) viability assay was performed using the Muse Annexin V & Dead Cell reagent (Merck Millipore), and RNA was extracted for RT-qPCR analysis using TRIzol reagent (Thermo Fischer Scientific, Inc.).

Quantitative analyses of mRNAs. For quantification of the relative mRNA content, 500 ng of total cellular RNA was reverse transcribed to cDNA with the Taq-Man Reverse Transcription Kit (cat no. N8080234; Applied Biosystems; Thermo Fisher Scientific, Inc.), as described by Gasparello *et al.* (24). qPCR experiments were performed using an assay consisting of a PCR primer pair and a fluorescently labeled 5' nuclease probe or SYBR Green. Assays IDs: i) Hs.PT.58.40226675 (HEX) for IL-6; ii) Hs.PT.58.38869678.g (Cy5) for IL-8; iii) Hs.PT.58.20610757 (FAM) for granulocyte-colony stimulation factor (G-CSF); iv) Hs.PT.58.38905484 (FAM) for NF- κ B p50; and v) Hs.PT.58.22880470 (FAM) for NF- κ B p65. The

primers and probes for ribosomal protein L13a (RPL13A) and b-actin and were as follows: β -actin forward, 5'-ACG ATGGAGGGGAAGACG-3' and reverse, 5'-ACAGAGCCT CGCCTTTG-3'; β -actin probe, 5'-5Cy5/CCTTGCACATGC CGGAGCC/3IAbRQSp/-3'; RPL13A forward, 5'-GGCAAT TTCTACAGAAACAAGTTG-3' and reverse, 5'-GTTTTG TGGGGCAGCATACC-3'; RPL13A probe, 5'-5HEX/CGC ACGGTC/ZEN/CGCCAGAAGAT/3IABkFQ/-3' (Applied Biosystems; Thermo Fisher Scientific, Inc.). The primers used for the amplification of BNT162b2 Spike sequences using a Master Mix with the SYBR Green intercalating Dye were forward 5'-CGAGGTGGCCAAGAATCTGA-3' and reverse, 5'-TAGGCTAAGCGTTTTGAGCTG-3', and β -actin forward 5'-CCTCGCCTTTGCCGATCC-3' and reverse, 5'-GGATCTTCATGAGGTAGTCAGTC-3' (Integrated DNA Technologies), according to Aldén *et al* (25). qPCR amplification of cDNA was performed at 95°C for 1 min, then 50 cycles of 95°C for 15 sec and 60°C for 1 min, using the CFX96 Touch Real-Time PCR Detection System (Bio-Rad Laboratories, Inc.). Relative expression was calculated using the comparative quantification cycle (Cq) method ($2^{-\Delta\Delta Cq}$ method) (26) and the endogenous controls human β -actin and RPL13A, used as normalizer. RT-qPCR reactions were performed in duplicate for both target and normalizer genes (24).

Computational studies. All the computational methodologies were performed on a 32 Core AMD Ryzen 93,905x, 3.5 GHz Linux Workstation (O.S. Ubuntu 20.04) equipped with GPU (Nvidia Quadro RTX 4000, 8 GB; Nvidia Corporation). The Toll-like receptor 4 (TLR4) dimer structure was derived from available information (27). The structure of S1PC was drawn and minimized using the Avogadro software (ver. 1.2.0; Avogadro Chemistry) (28). A blind docking simulation was performed on the entire TLR4 dimer surface using the AutoDock Vina software (ver. 1.2.3; Center for Computational Structural Biology) (29). The top scoring complex was submitted to all-atom unbiased molecular dynamics (MDs) simulation, as described by Zurlo *et al* (22), using the GROMACS ver. 2025.1 software, open source (30), patched with Plumed ver. 2.6.5 (31) under the Charmm36 force field (32). The complex was included in a rectangular box of 8x10x7 nm length, solvated and neutralized using 0.15 M sodium chloride. The full system was submitted to energy minimization and equilibrated under constant temperature and volume and constant temperature and pressure (NPT) conditions. Long-range electrostatic interactions were modelled using the Particle Mesh Ewald algorithm (33). The LINCS (34), Nosé-Hoover (35) and Parrinello and Rahman (36) algorithms were used in the simulations for restraints and as thermostat and barostat, respectively. MDs were conducted under the NPT conditions for 50 nsec with 2 fsec time steps. Root-mean-squared deviation (RMSD), root-mean-squared fluctuation, number of hydrogen bonds and interaction energy were obtained through the 'rms', 'rmsf', 'hbond' and 'energy' routines implemented in GROMACS.

Cell viability assay. Effects on cellular viability and apoptosis Annexin V and Dead Cell assay were performed using the flow cytometry-based Muse Cell Analyzer (Merck Millipore) instrument, according to the protocols supplied by the

manufacturer. Cells were washed with sterile DPBS 1X, trypsinized, and 150,000 cells were suspended in LHC-8 medium and diluted (1:2) with Muse Annexin V & Dead Cell reagent (Annexin V-PE and 7-AAD) (Merck Millipore) and analyzed. After an incubation of 15 min at room temperature in the dark, samples were acquired and data were analysed using the Muse 1.5 Analysis Software with the Annexin V and Dead Cell Software Module (Merck Millipore) (37).

Western blotting. For NF- κ B (p105/p50 and p65) protein quantification, 20 μ g total protein extract in RIPA Buffer (Thermo Fisher Scientific, Inc.) quantified with BCA kit (Pierce; Thermo Fisher Scientific, Inc.) were denatured for 5 min at 98°C and loaded onto a SDS polyacrylamide (8%) gel in Tris-glycine buffer (25 mM Tris, 192 mM glycine and 0.1% SDS). The electrotransfer to 0.2- μ m nitrocellulose membranes was performed overnight at 360 mA and 4°C in electrotransfer with CAPS buffer (25 mM Tris, 192 mM glycine, CAPS 10 mM and 10% methanol). Obtained membranes were stained in Ponceau S solution (Sigma-Aldrich; Merck KGaA) to verify proteins transfer and incubated in 25 ml blocking buffer (TBS-T with 5% nonfat dry milk (Cell Signalling Technology, Inc.) for 1 h at room temperature. After three washes in TBS-T 1X (containing Tween-20 at 0.1%), membranes were incubated overnight at 4°C in primary antibodies (NF- κ B p105/p50 Ab; cat. no. GTX133711; 1:5,000 dilution; GeneTex, Inc.). The day after, membranes were washed in TBST 1X and incubated for 1 h at room temperature, with an appropriate HRP-conjugated secondary antibody (anti-rabbit IgG HRP-conjugated; cat. no. 7074P3; 1:2,000 dilution; Cell Signalling Technology, Inc.). β -actin (primary antibody: Cat. no. 4970S; 1:1,000; Cell Signalling Technology, Inc.) was used as a normalization control. After incubation with the ECL Solution (Claitry™ ECL Substrate; Bio-Rad Laboratories, Inc.) the gel images were acquired with the ChemiDoc (Bio-Rad Laboratories, Inc.) with the software Image Lab version 6.1.0, used also for densitometric analysis (Bio-Rad Laboratories, Inc.).

Analysis of cytokines, chemokines and growth factors. Proteins released into culture supernatants were measured using Bio-Plex Human Cytokine 27-plex Assay (cat. no. M500KCAF0Y; Bio-Rad Laboratories, Inc.), as suggested by the manufacturer. The assay allows the multiplexed quantitative measurement of 27 cytokines/chemokines [including FGF basic, Eotaxin, G-CSF, granulocyte macrophage-colony stimulating factor, IFN- γ , IL-1 β , IL-1ra, IL-2, IL-4, IL-5, IL-6, IL-7, IL-8, IL-9, IL-10, IL-12 (p70), IL-13, IL-15, IL-17A, C-X-C motif chemokine ligand 10, chemokine ligand (CCL)2, CCL3, CCL4, PDGFBB, CCL5, TNF- α and VEGF] in a single well (21).

Briefly, an amount of 50 μ l cytokine standards or samples (diluted supernatants recovered from IB3-1 cells) was incubated with 50 μ l anti-cytokine conjugated beads in a 96-well filter plate for 30 min at room temperature with shaking. The plate was washed by vacuum filtration three times with 100 μ l Bio-Plex Wash Buffer, 25 μ l diluted detection antibody was added to each well and the plate was incubated for 30 min at room temperature with shaking. After three filter washes, 50 μ l streptavidin-phycoerythrin was added and the plate was incubated for 10 min at room temperature with shaking.

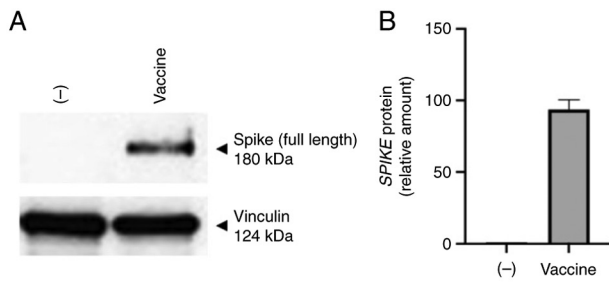


Figure 1. Production of severe acute respiratory syndrome coronavirus 2 spike protein by IB3-1 cells treated with the BNT162b2 vaccine. (A) Representative western blot images and (B) corresponding semi-quantitative analysis of independent experiments ($n=3$) normalized using vinculin as internal standard. (-) Untreated samples. The uncropped original version of the western blot images shown in this figure can be found in Fig. S1.

Finally, the plate was washed by vacuum filtration three times, the beads were suspended in Bio-Plex Assay Buffer and the plate was read by a Bio-Rad 96-well plate reader. Collected data were analyzed by the Bio-Plex Manager Software (version 6.2; Bio-Rad Laboratories, Inc.) (21).

Statistical analysis. The data are presented as the mean \pm standard deviation of at least three independent experiments. Statistical differences between/among groups were analyzed using one-way ANOVA. Prism (v. 9.02) by GraphPad software (Dotmatics) was used (followed by Bonferroni's test). $P < 0.05$ was considered to indicate a significant difference.

Results

Preliminary characterization of the bronchial epithelial IB3-1 cellular system after exposure to the COVID-19 BNT162b2 vaccine. The effects of exposure of IB3-1 cells to the COVID-19 BNT162b2 vaccine (22) were first analyzed. After the treatment, total cellular RNA was extracted for RT-qPCR analysis, whereas culture supernatants were isolated for the analysis of secreted proteins, to characterize BNT162b2-induced alteration of the secretome profile. IB3-1 cells treated with BNT162b2 vaccine were found to produce large amounts of SARS-CoV-2 Spike protein. To obtain this information, western blotting was performed using protein extracts from IB3-1 cells treated with the BNT162b2 vaccine (Fig. 1). A concentration of $0.5 \mu\text{g/ml}$ of BNT162b2 was found to be sufficient to induce S-protein (Figs. 1, S1 and S2) and cytokine and chemokine production (Fig. S3), with lower inhibitory effects on cell viability compared with 1 and $2 \mu\text{g/ml}$ of BNT162b2 (22). The western blotting data shown in Fig. 1 confirm that S-protein is produced by BNT162b2 treated cells, which was reported elsewhere in other cellular model systems (22,38,39). In addition, IB3-1 cells treated with the BNT162b2 vaccine were found to accumulate large amounts of SARS-CoV-2 Spike mRNA (Fig. S2) as discussed elsewhere (40). This suggests that the Spike protein was expressed by IB3-1 cells treated with the BNT162b2 vaccine. When RT-qPCR and Bio-plex analyses were performed using RNA or secreted materials from BNT162b2-treated IB3-1 cells, it was found that they exhibited the increased expression and production

of pro-inflammatory factors, including IL-6, IL-8, G-CSF, GM-CSF and IP-10 (Figs. S3 and S4).

GC-MS analysis of SIPC. Fig. 2 shows the GC-MS analysis of SIPC as a di-TBDMS derivative. Both the total ion current (TIC) chromatogram and the selected ion chromatogram (SIM) are shown. Fig. 2A and B revealed the presence of two partially co-eluting peaks at 10.55 and 10.57 min (Fig. 2B), exhibiting identical electron impact mass spectra (Fig. 2C) and the corresponding cis- and trans-isomers of SIPC. Both cis- and trans-SIPC have previously been identified in AGE, with the cis-form believed to be generated through isomerization of its trans form (41). Furthermore, the GC-MS analyses presented in Fig. 2 confirmed the purity levels of the SIPC preparation procedure, which was found to be $>95\%$.

SIPC inhibits NF- κ B expression in IB3-1 cells treated with the BNT162b2 vaccine. Considering the effects of the spike protein on the NF- κ B pathway (42-44), RT-qPCR was next performed to measure p50 and p65 mRNA expression in BNT162b2-treated IB3-1 cells (Fig. 3), following on from a previous study on the same system using SARS-CoV-2 spike protein (45). Cells were therefore exposed for 24 h to BNT162b2 and then cultured for an additional 48 h in the presence of increasing concentrations of SIPC.

In total, two important conclusions could be gathered from the results shown in Fig. 3. BNT162b2 stimulated the accumulation of NF- κ B p50 (Fig. 3A) and NF- κ B p65 (Fig. 3B) mRNA expression, even though NF- κ B was already present at high concentrations in the cytoplasm of IB3-1 cells before BNT162b2 treatment (21,45). In addition, after the BNT162b2-treated IB3-1 cells were cultured with SIPC, reversal of the accumulation of NF- κ B p50 (Fig. 3A) and NF- κ B p65 (Fig. 3B) mRNA expression was observed. The effect of SIPC resembled that observed using the NF- κ B inhibitor sulforaphane (46) on the IB3-1 cellular model system (45). In agreement with the results shown in Fig. 3, the effects of 50 mM SIPC on NF- κ B were also evident on protein level according to the western blot analysis using an antibody recognizing the p50/p105 NF- κ B subunits (Fig. S5).

SIPC inhibits the accumulation of proinflammatory mRNAs in IB3-1 cells treated with the BNT162b2 vaccine. To verify if the BNT162b2-induced production of proinflammatory mRNA expression could be affected in IB3-1 cells treated with the BNT162b2 vaccine in the presence of SIPC, RT-qPCR analysis was performed (Fig. 4). The BNT162b2 vaccine was used at $0.5 \mu\text{g/ml}$ to minimize its anti-proliferative effects (22). Analysis of mRNA accumulation was performed 48 h after treatment. IL-1 β , IL-6 and IL-8 (47), G-CSF (48) and GM-CSF (49) were first considered, before experimentally focusing on IL-6, IL-8 and G-CSF, which are much more expressed in the IB3-1 experimental model system employed as reported by Gasparello *et al.* (21,45).

The results shown in Fig. 4 demonstrate that the expression of IL-6 (Fig. 4A), IL-8 (Fig. 4B) and G-CSF (Fig. 4C) mRNA expression was significantly upregulated in IB3-1 cells after exposure to the BNT162b2 vaccine. The BNT162b2-mediated induction of expression was more efficient compared with that of SARS-CoV-2 Spike protein (Fig. S4 and data not shown). No major changes in the accumulation of mRNA expression

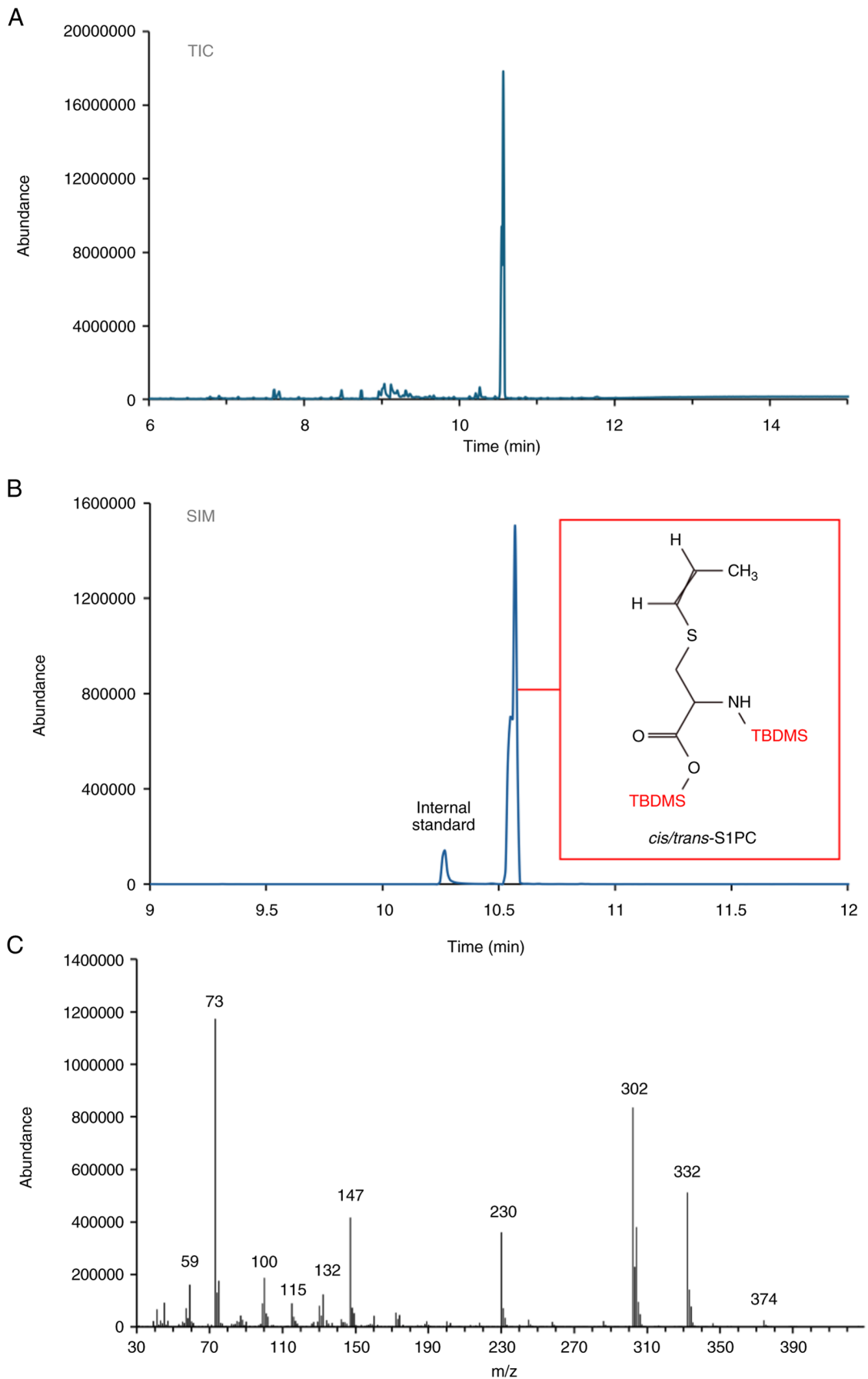


Figure 2. Gas chromatography-mass spectrometry results analysis of S1PC. (A) TIC chromatogram of S1PC derivatized with TBDMS. (B) SIM of the sample derivatized with TBDMS acquiring the following ions: m/z 239 (3,4-dimethoxybenzoic acid, the internal standard) and m/z 332 (S1PC). (C) electron ionization mass spectrum of *cis/trans*-S1PC as di-TBDMS derivative. S1PC, S-1-propenyl-L-cysteine; TIC, total ion current; SIM, selected ion chromatogram; TBDMS, tert-butyldimethylsilyl-; m/z, mass-to-charge ratio.

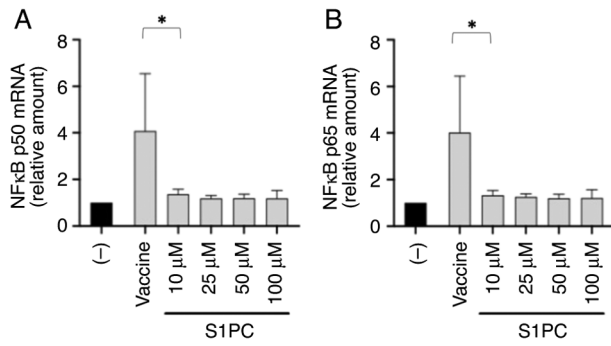


Figure 3. Effects of increasing concentrations of S1PC on BNT162b2-induced accumulation of NF- κ B expression. Expression of (A) p50 and (B) p65 mRNA. The mRNA expression was analyzed by reverse transcription-quantitative PCR using IB3-1 cells exposed to 1 mg/ml BNT162b2 and treated for 72 h. * $P < 0.05$. Relative expression was calculated using the $2^{-\Delta\Delta C_t}$ method and the endogenous control human β -actin was used for normalization (22). S1PC, S-1-propenyl-L-cysteine.

of RPL13A were observed. The RPL13A mRNA was studied, due to its role in mitochondrial metabolism and that its expression is highly stable in several cellular systems (50,51).

The effects of different concentrations (range 1-100 μ M) of S1PC on BNT162b2-stimulated IB3-1 cells were next studied by RT-qPCR, using β -actin as internal control (Fig. 4). A concentration-dependent inhibition of the accumulation of IL-6 (Fig. 4A), IL-8 (Fig. 4B) and G-CSF (Fig. 4C) mRNAs was detectable, suggesting that 10 μ M S1PC is sufficient to inhibit to some extent the expression of IL-6, IL-8 and G-CSF induced in these cells by the BNT162b2 vaccine. However, higher S1PC concentrations were found to be more effective. By contrast, no inhibitory effects were observed in the RPL13A mRNA expression levels (Fig. 4D).

The results shown in Fig. 4 indicate that S1PC can be proposed as an anti-inflammatory component of AGE to be considered in pre-clinical studies (52,53). However, further studies on the biological effects of S1PC are required to assess possible anti-proliferative and/or cytotoxic effects associated with the inhibition of proinflammatory gene expression.

Effects of S-1-propenyl-L-cysteine on BNT162b2 treated IB3-1 cells: analysis of cell proliferation efficiency and cell viability. To analyze in depth the effects of S1PC on cell viability, the proportion of live/dead cells was analyzed using the MUSE[®] Annexin V & Dead Cell Kit, which was used to discriminate among live cells, apoptotic cells and dead cells (24,37).

The results obtained are shown in Fig. 5. Fig. 5A shows that treatment of IB3-1 cells with the BNT162b2 vaccine is associated with the reduction of cell viability, whereas S1PC did not induce anti-proliferative effects in IB3-1 cells treated with 0.5 μ g/ml of the BNT162b2 vaccine. In addition, Fig. 5B-D indicates that treatment of IB3-1 cells with the BNT162b2 vaccine is associated with a decrease of the % live cells (Fig. 5B) and an increase of the % of dead cells (Fig. 5C). No major effects of S1PC on % live cells or % dead cells could be observed (Fig. 5B and C).

Molecular docking and molecular dynamics support the hypothesis that S-1-propenyl-L-cysteine efficiently interacts with TLR4. To propose the possible mechanism of action

of S1PC, a molecular docking analysis was performed. Preliminary analyses demonstrated a lack of binding of S1PC to NF- κ B. The binding of low-molecular-weight drugs to this protein has however been previously reported, such as trimethylangelicin and analogues (54), corilagin (55) and sulforaphane (45,47). In these cases, efficient interactions with NF- κ B were found. However, no evidence of molecular interaction between S1PC and NF- κ B could be found in the present docking analysis (data not shown). Since TLR are upstream regulators of the NF- κ B signaling (56-58), the possible interaction between S1PC and TLR4 was assessed using the docking AutoDock Vina software (Fig. 6) (29). The results obtained indicate that S1PC is able to bind *in silico* that to the Toll-IL-1 receptor domain of TLR4. The amino acids involved in the S1PC-TLR4 interactions are His685, Val655, Arg722 and Tyr657.

To further sustain the reliability of the molecular interaction reported in Fig. 6, the computed model was submitted to 50 nsec of all-atom unbiased molecular dynamics simulation. The results obtained demonstrated that the complex remained stable, as can be seen from the C α -RMSD values calculated over the simulation time (Fig. 7A). In particular, the hydrogen bonds reported in Fig. 7B were retained during the entire molecular dynamic's simulation, yielding an estimated interaction energy of -65.2 ± 7.3 Kcal/mol (computed as the sum of short-range Lennard-Jones and short-range Coulomb contributions over the 50 nsec of simulation). In addition, binding with S1PC was found to reduce the intermolecular interaction between the TLR4 domains, as revealed by both the reduction in H-bond numbers (Fig. 7B) and the increased per-residue RMSF values in comparison to the apo complex (Fig. 7C-E).

Discussion

One of the most important and clinically relevant characteristics of COVID-19 is the high expression of IL-6, IL-8 and several other cytokines, chemokines and growth factors (2). This is frequently associated with a hyperinflammatory state and severe forms of COVID-19 (59). Del Valle *et al* (60) previously reported that high serum IL-6, IL-8 and TNF- α levels at the time of hospitalization are associated with poor prognosis. In another study, Burke *et al* (61) also found that increased IL-6 and IL-8 levels can be used to predict clinical outcomes in patients with COVID-19. Therefore, anti-inflammatory molecules and novel anti-inflammatory strategies are highly needed.

In the present study, the human bronchial epithelial IB3-1 cell line was used, where it was stimulated by the COVID-19 BNT-162b2 vaccine to express proinflammatory factors. The IB3-1 cell line has been previously used to study the inflammatory response (62-64) and effects of anti-inflammatory agents on the expression of proinflammatory genes known to be involved in COVID-19 cytokine Storm (21,45,54,55,65).

The main aim of the present study was to determine the possible effects of a major component of AGE, S1PC, on the expression of proinflammatory factors and hypothesize the possible mechanism of action. The beneficial effects of garlic have been previously reported, where they were proposed to be due to the presence of several bioactive molecules within its

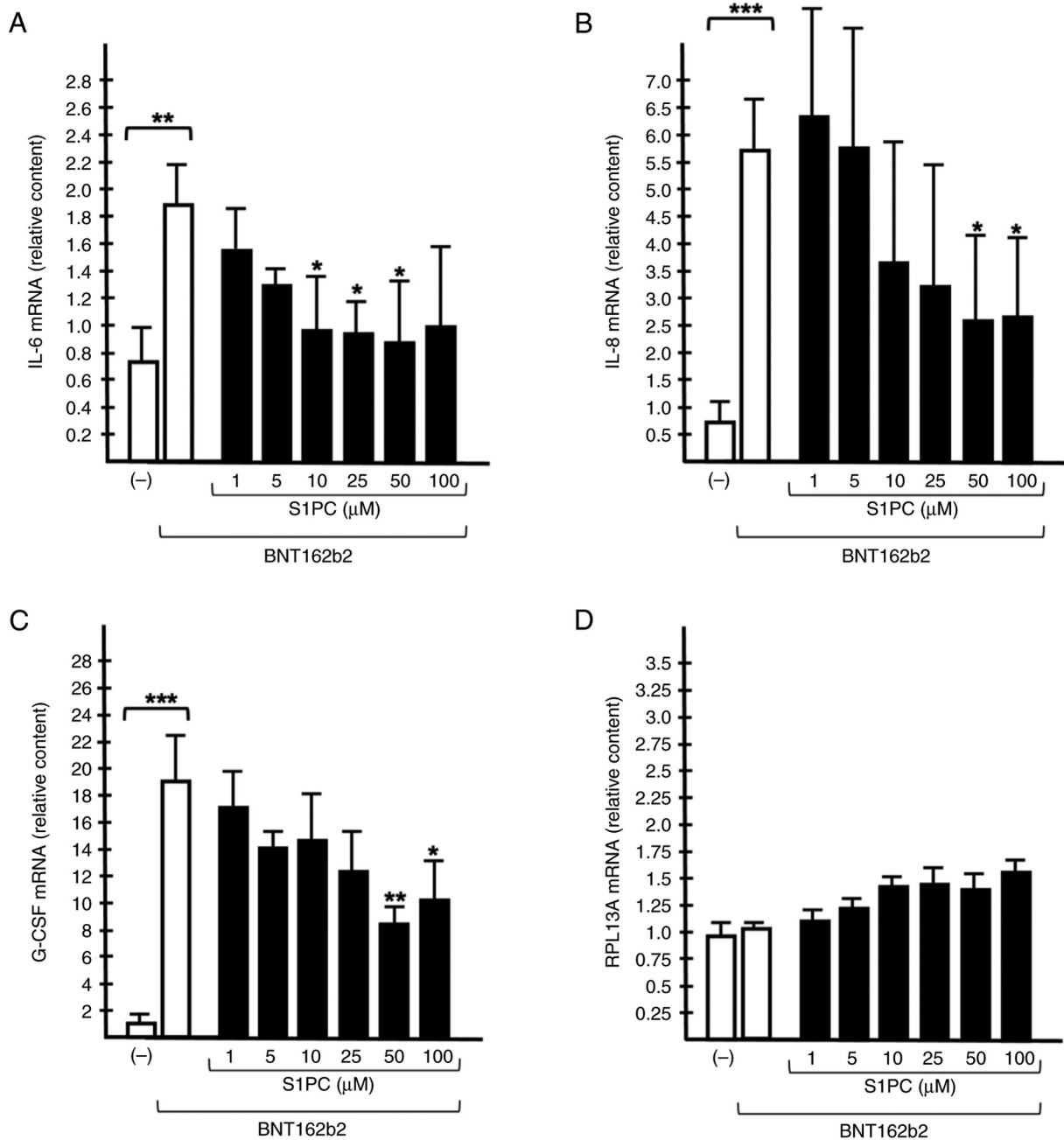


Figure 4. Effects of increasing concentrations of S1PC on the elevation of proinflammatory mRNA expression in BNT162b2-stimulated IB3-1 cells. White histograms represent the effects of 0.5 μg/ml of BNT162b2 vaccine on (A) IL-6, (B) IL-8, (C) G-CSF and (D) RPL13A mRNA content. Reverse transcription-quantitative PCR was performed 48 h after treatment. Black histograms represent the effects of increasing concentrations of S1PC on BNT162b2 treated IB3-1 cells. Cells were exposed to 0.5 μg/ml of BNT162b2 vaccine and treated with the indicated concentrations of S1PC. Results represent the means ± standard deviation. *P<0.05, **P<0.01 and ***P<0.001 from four independent experiments. Relative expression was calculated using the 2^{-ΔΔC_q} method and the endogenous control human β-actin was used for normalization. S1PC, S-1-propenyl-L-cysteine; G-CSF, granulocyte-colony stimulation factor; RPL13A, ribosomal protein L13a.

preparations, including lipid-soluble allyl sulfur compounds and water-soluble derivatives, such as SAC and S1PC (66). S1PC is a stereoisomer of SAC (17). This sulfur-containing amino acid has important properties for the beneficial pharmacological roles of AGE (20). S1PC is present only in trace amounts in raw garlic, but its concentration will increase, approaching that of SAC levels, during the aging process of AGE (41). S1PC has been observed to show immunomodulatory functions both *in vitro* and *in vivo*, in addition to reduce blood pressure in a hypertensive animal model (67,68). In

addition, a previous pharmacokinetic investigation showed that S1PC is rapidly absorbed after oral administration in rats and dogs, with high bioavailability (~100%) (17). In addition, S1PC exhibited a low inhibitory effect on human cytochrome P450 activities, even when it was used at a concentration of 1 mM (67,68). Considering all these findings regarding the potential medicinal value of S1PC, this molecule was suggested to be another pharmacologically active and safe derivative of AGE similar to SAC, consistent with the proposal made by Kodera *et al* (17).

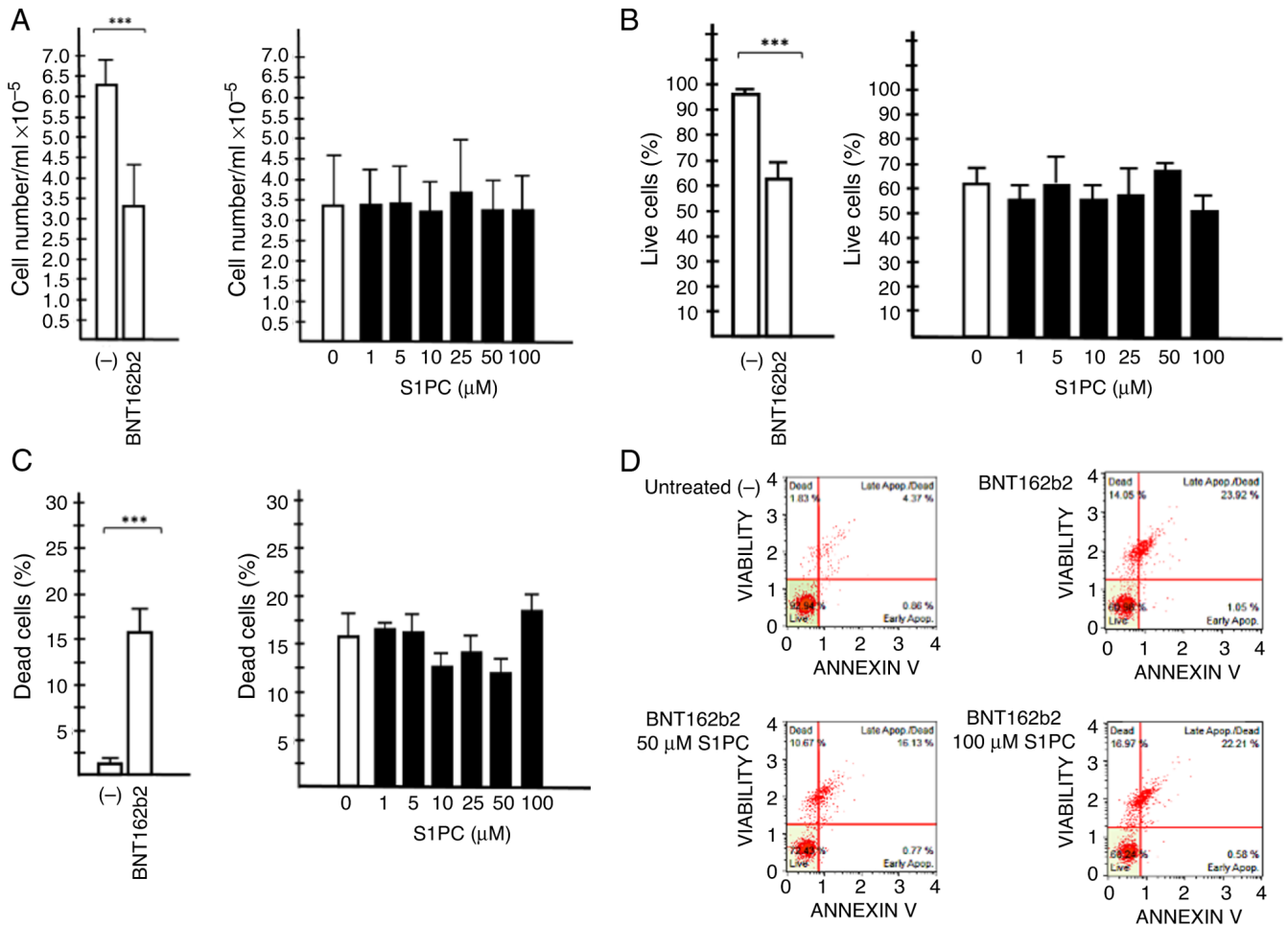


Figure 5. Effects of SIPC on viability of BNT162b2 treated cells. Effects of 0.5 μ g/ml of BNT162b2 vaccine and increasing concentrations of SIPC on BNT162b2 treated IB3-1 cells on (A) cell proliferation, (B) viability and (C) toxicity. Cells were exposed to 0.5 μ g/ml of BNT162b2 vaccine and treated with the indicated concentrations of SIPC. Cell number and % of live and dead cells were evaluated after 48 h cell culture as described in the Materials and methods section. Viability and toxicity were analyzed using the MUSE[®] Annexin V & Dead Cell Kit. (D) Representative FACS analyses relative to panels B-C. Results of panels A, B and C represent the means \pm standard deviation of three independent experiments. *** P <0.001. SIPC, S-1-propenyl-L-cysteine.

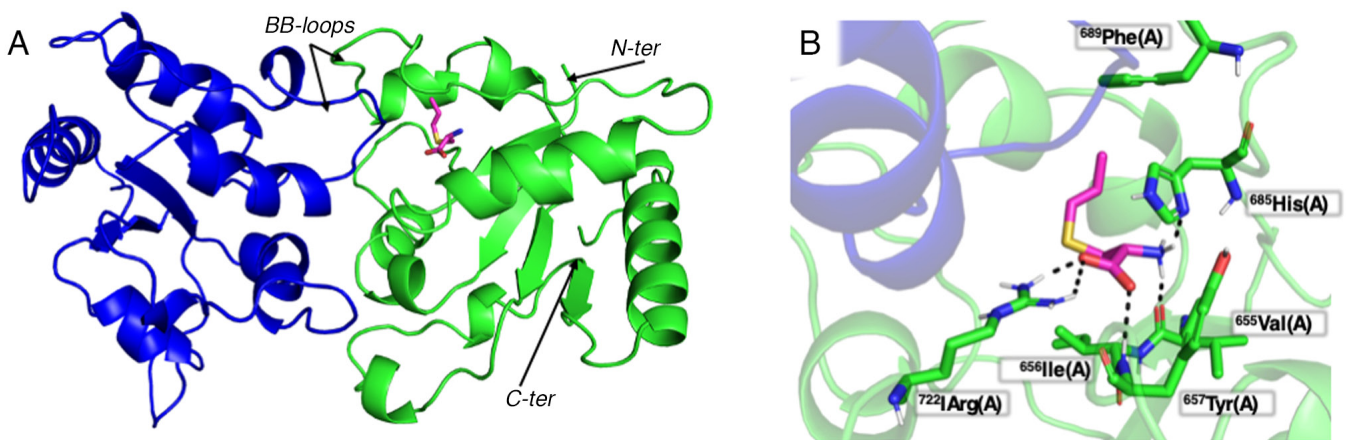


Figure 6. Simulation of SIPC binding to TLR4. Binding mode predicted for SIPC with the (A) TLR4-Toll-IL-1 receptor dimer and (B) details of interactions. TLR4 monomers are depicted in green and blue respectively; SIPC is depicted as stick (magenta colored carbon). Hydrogen bonds are depicted as dashed black lines. SIPC, S-1-propenyl-L-cysteine; TLR4, Toll-like receptor 4.

The present GC/MS analysis confirmed that the SIPC preparation contains both *cis*- and *trans*-isomers of SIPC. Concerning the biological activity of the applied SIPC

preparation, the results presented in the present study suggest that the release of key proteins of the COVID-19 'cytokine storm' (69) can be inhibited by SIPC. Since control of this

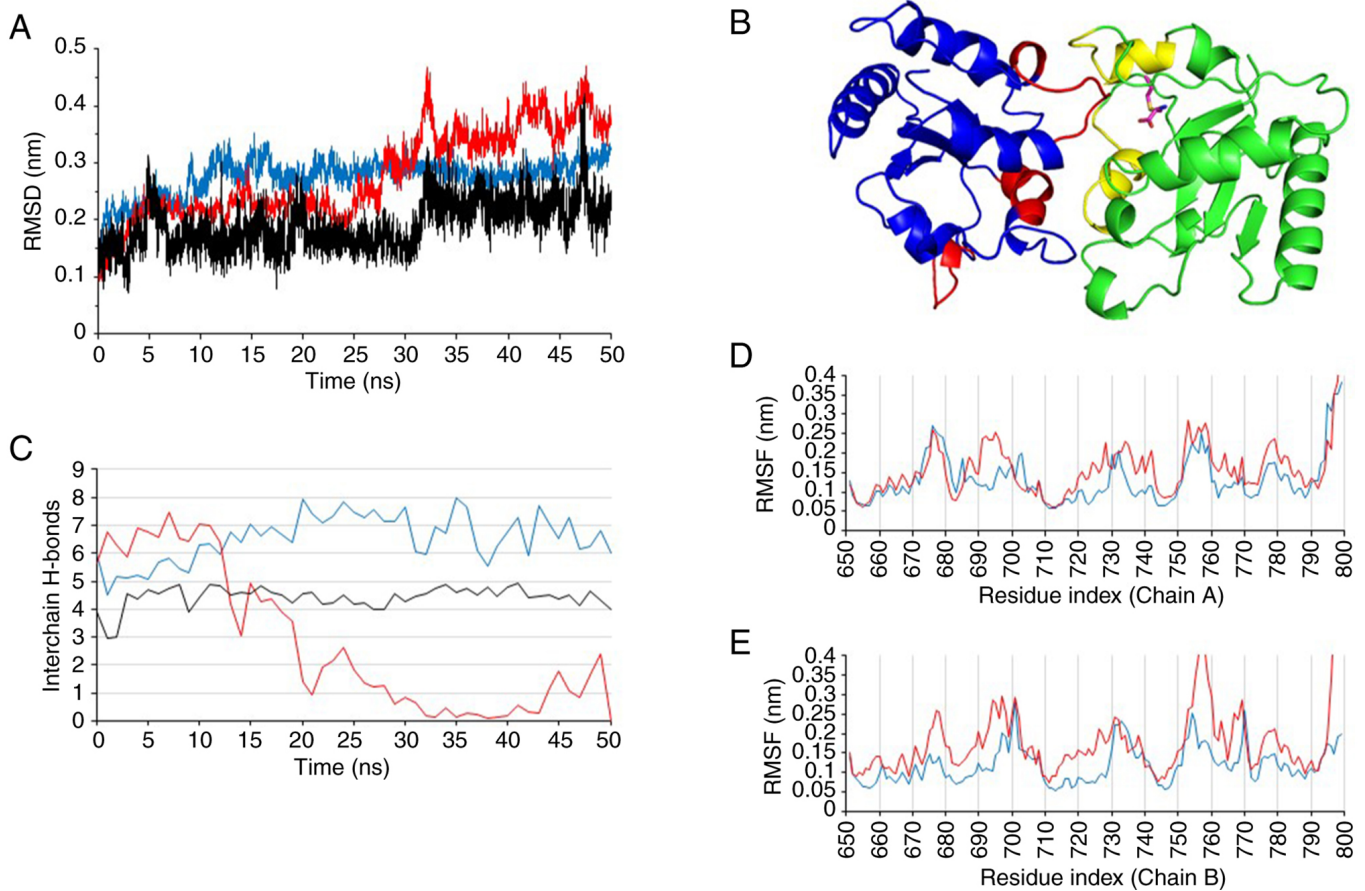


Figure 7. Summary of molecular dynamics results. (A) α -RMSD (nm) was calculated for apo-TLR4 dimer (blue line) and for TLR4-dimer in complex with SIPC (red line). The heavy atoms-RMSD for SIPC are also reported (black line) showing a stable complex. (B) TLR4/TLR4/SIPC complex coloured as function of the largest per-residue RMSF (yellow residues for TLR4-chain A; red residues for TLR4-chain B). (C) Intermolecular H-bonds formed between TLR4 chains in apo (blue line) and in complex with SIPC (red line) dimers. Note that when complexed with SIPC, the TLR4 monomer binding is strongly destabilized. The H-bonds formed between SIPC and the TLR4 chain A are also reported (black line). RMSF values are reported in detail for (D) chain A and (E) chain B. In both cases, blue lines represent the RMSF values computed for the apo dimer and red lines indicate the RMSF values computed for the ternary complex. RMSD, root-mean-squared deviation; RMSF, root-mean-squared fluctuation; SIPC, S-1-propenyl-L-cysteine; TLR4, Toll-like receptor 4.

'cytokine storm' is a major issue in the management of patients with COVID-19 (70), results from the present study may stimulate the development of protocols for controlling the hyperinflammatory state associated with SARS-CoV-2 infection. In addition, experimental activity on plant extracts and food supplements containing SIPC for supporting the possibility of using 'phyto-preparations' in combination with 'conventional' medicine focusing on COVID-19 treatment is encouraged as a result of the present study. The present study also extended recent observations by Gasparello *et al* (71) on the effects of AGE and its component SAC on expression of pro-inflammatory genes. In the present study, SIPC was considered for the first time and G-CSF was included in the analysis, sustaining the conclusions of the previous study on AGE and SAC (71), suggesting an inhibitory effect of these agents on the expression of pro-inflammatory genes. To the best of our knowledge, the present study was the first to consider potential cytotoxicity and anti-proliferative effects of an AGE component on bronchial epithelial cells exposed to

the BNT162b2 vaccine. In addition, in the present study low concentrations (1 and 5 μ M) of the AGE component SIPC were considered.

One of the limitations of the present study is the lack of a full explanation on the mechanism of action of SIPC. This should be considered in future research plans, since it can be used to identify novel targets for therapeutic strategies. Among the several possibilities, SIPC can exert its anti-inflammatory activity by inhibiting the JNK/activator protein-1 (AP-1)/NF- κ B pathway. This may be associated with the activity of TLRs, such as TLR4 (72-74). The present study supports the hypothesis that SIPC interacts with and possibly inhibits TLR4, by destabilizing the dimer interactions. TLRs (including TLR4) are involved in SARS-CoV-2 entry into infected cells (75,76) and in NF- κ B expression (77,78). Therefore, it can be hypothesized that inhibitors of TLR4 can inhibit the early phases of SARS-CoV-2 infection, including activation of the NF- κ B pathway. The inhibition of NF- κ B by SIPC may be relevant in the context of possible inhibition by SIPC of proinflammatory

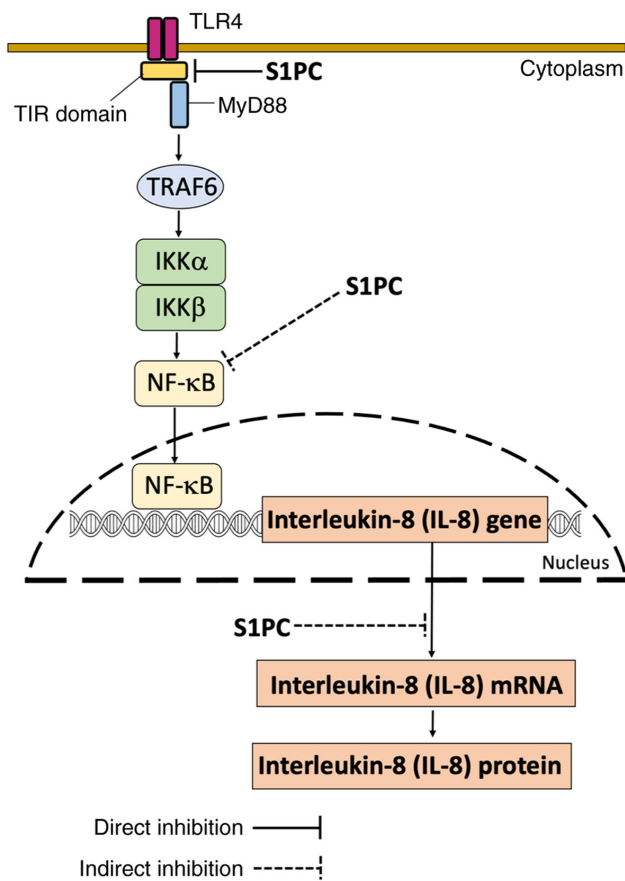


Figure 8. Proposed mechanism of action of S1PC. Indirect inhibition of NF- κ B may be caused by a direct interaction/inhibition of S-allyl-L-cysteine and S1PC with TLR4 (and/or other TLRs, including intracellular TLRs). NF- κ B inhibition is causative of the inhibitory effects of NF- κ B-regulated genes, such as IL-1 β , IL-6 and IL-8. S1PC, S-1-propenyl-L-cysteine; TLR4, Toll-like receptor 4; TIR, Toll-IL-1 receptor; MyD88, myeloid differentiation primary response 88; TRAF6, TNF receptor associated factor 6.

genes, which contain NF- κ B binding sites in their promoter sequence. The effect of S1PC resembled that observed using the NF- κ B inhibitor sulforaphane (46) on the IB3-1 cellular model system (45,47). The present study supports the hypothesis that TLR-4 should be considered as a target of anti-SARS-CoV-2 therapeutic strategies (78,79). In particular, Yang *et al* (80) previously showed that an aptamer blocking the Spike-TLR4 interaction is able to selectively inhibit SARS-CoV-2-induced inflammation. Docking data from the present study sustained this hypothesis, which showed *in silico* that S1PC is possibly able to bind to the Toll-IL-1 receptor domain of TLR4. The amino acids involved in the S1PC-TLR4 interactions are His685, Val655, Arg722 and Tyr657, belonging to a TLR4 region, serving a role in the molecular interaction with the SARS-CoV-2 Spike protein (81). Therefore, S1PC should be considered in further studies aimed at verifying its possible anti-SARS-CoV-2 activity.

In conclusion, a simple experimental model system was developed and validated for the identification and characterization of molecules able to inhibit the expression of genes involved in the COVID-19 'cytokine storm' in the present study. Specifically, exposure of epithelial IB3-1 cells to the COVID-19 BNT162b2 vaccine is associated with a potent increase in the expression of the transcription factor NF- κ B

and NF- κ B-regulated genes, including IL-6, IL-8 and G-CSF. However, the present study did not explain the mechanism of action of BNT162b2 in inducing the upregulation of proinflammatory gene expression. The activity of BNT162b2 may be due to the liposomal vaccine vector, to the Spike mRNA or both of these BNT162b2 components. Lipid-based RNA nanoparticles can stimulate inflammatory responses (82-84), whereas the purified SARS-CoV-2 spike protein (encoded by the BNT162b2 mRNA vaccine) can also induce the upregulation of proinflammatory gene expression, despite to an extent lower compared with BNT162b2. Therefore, both lipid formulation and spike RNAs can contribute to the activity of BNT162b2 on the expression of proinflammatory genes.

Treatment with S1PC was not found to be toxic but it reversed the proinflammatory cytokine IL-6, IL-8 and G-CSF upregulation induced by the BNT162b2 vaccine in IB3-1 cells. Considering the TLR4-NF- κ B interplay, molecular dynamic results obtained in the present study suggest that the anti-inflammatory effects of S1PC may be due to an inhibition of the JNK/AP-1/NF- κ B interaction. Therefore, S1PC should be further evaluated as a potential inhibitor of proinflammatory factors involved in the COVID-19 'cytokine storm', moving the study from *in vitro* experimental model systems to *in vivo* treatments (80-85) and clinical trials. Examples of clinical trials based on AGE and reporting anti-inflammatory effects are those published by Wlosinska *et al* (86) and by Xu *et al* (87). Although *in vitro* experimental systems are viable for the analysis of short-term effects, studies using *in vivo* systems and clinical trials are needed to study long-term effects, including potential negative effects.

The present study has several limits that should be considered in future studies. Only one cell line has been studied (the bronchial epithelial IB3-1 cell line). Exposure of IB3-1 cells to the BNT162b2 vaccine should be just considered as a simple method to induce the increased expression of proinflammatory genes to an extent higher than that exhibited by SARS-CoV2 Spike-treated IB3-1 cells (45,47). The possible inhibitory effects of S1PC on other experimental model systems closely resembling the cell types that are involved in the COVID-19 cytokine storm, such as T cells, macrophages, monocytes, dendritic cells and endothelial cells, should also be investigated (3-5). In addition, other well validated experimental systems mimicking the induced proinflammatory state can be employed, such as the same IB3-1 exposed to *Pseudomonas aeruginosa* (88), to TNF- α (54,55) or to lipopolysaccharide (89). In all of these aforementioned experimental model systems, cytokines and chemokines involved in COVID-19 cytokine storm were found to be upregulated, including IL-6 and IL-8 (54,55,88,89). Furthermore, other model systems have been proposed, based on the *Pseudomonas aeruginosa* infection of other cell lines, such as NuLi (88), CuFi (88-90) and A549 (91). Furthermore, experiments performed on skeletal muscle cells exposed to the BNT162b2 vaccine and on SARS-CoV-2-infected lung epithelial Calu-3 cells (47) can be considered to closely mimic the vaccination procedure by intramuscular administration (92) and COVID-19 lung infection, respectively. A possible inhibitory effect of S1PC on NF- κ B signaling in SARS-CoV-2-infected lung epithelial cells should be considered, as it was previously reported using the NF- κ B inhibitor sulforaphane (45,47).

Another limitation of the present study is that possible negative effects on gene expression of SIPC have not been considered. Global transcriptomic and proteomic analyses will be necessary to clarify this point. In terms of the docking and molecular dynamics experiments, a proposed model of possible interactions between SIPC and TLR4, along with their effects on TLR4 functions, was constructed (Fig. 8). It must be emphasized that it is a speculative model at this stage, where further experimental work based on biochemical evidence validating the predicted SIPC-TLR4 interaction and its effects on downstream TLR4 signaling is encouraged. The effects of the SIPC homologue SAC on TLR4 have been also reported previously (93,94). An extensive study of AGE constituents (SAC and SIPC) on other members of the TLR family are highly warranted. In addition, further experimental effort is needed to identify other agents within the list of AGE components that can modify gene expression induced by the COVID-19 BNT162b2 vaccine. This is to verify whether combined treatment with SIPC could be possible to obtain the highest inhibitory effects, using also SARS-CoV-2 infected cells.

In conclusion, the present study should encourage further experiments based on western blotting and Bio-plex analyses to verify whether the inhibitory effects of SIPC on the accumulation of NF- κ B and proinflammatory mRNAs are associated with a decrease of proinflammatory protein production and release. This will clarify the clinical impact of the present study. In addition, possible validation in clinical trials should be considered, given the potential relevance of the present study for COVID-19 management. Furthermore, the present study has clinical relevance, considering the role of inflammation in lung pathologies, such as cystic fibrosis, asthma and COPD (95-97), in neurological diseases (98), in osteoarthritis (53) and in skeletal muscular atrophy (94-99), cardiovascular diseases (100), diabetes (101) and cancer (102,103).

Acknowledgements

The authors would like to thank Dr Takahiro Ogawa and Dr Toshiaki Matsutomo (Wakunaga Pharmaceutical Co., Ltd.) for organizing the shipment of SIPC.

Funding

The present study was funded by the MUR-FISR COVID-miRNAPNA Project (grant no. FISR2020IP_04128), by FIRD 2024 funds from the University of Ferrara (grant no. FIRD-Finotti 2024), by the Interuniversity Consortium for Biotechnologies, Italy (grant no. CIB-Unife-2020) and by Wakunaga Pharmaceutical Co. Ltd. (grant no. IPFO2024).

Availability of data and materials

The data generated in the present study may be requested from the corresponding author.

Authors' contributions

AF, EA and RG designed the experimental plan. CP, JG, MZ, FDP and AF were involved in the methodology development.

CP, JG, GM, AM, MZ, FDP and PF performed the experiments. CP and FDP performed the treatments, the western blotting and the reverse transcription-quantitative PCR analyses. JG and MZ developed and characterized the experimental model system based on exposure of IB3-1 cells to the BNT162b2 vaccine. FDP and AF performed the cytotoxicity tests. EA, AM and PF performed the gas chromatography-mass spectrometry analyses. GM performed the molecular docking and molecular dynamics experiments. AF, CP, JG and RG curated the data and analyzed the results. RG wrote the original draft. AF, RG and EA reviewed and edited the draft. All authors read and approved the final version of the manuscript. RG and AF confirm the authenticity of all the raw data.

Ethics approval and consent to participate

Not applicable.

Patient consent for publication

Not applicable.

Competing interests

The authors declare that they have no competing interests.

References

- Pascarella G, Strumia A, Piliago C, Bruno F, Del Buono R, Costa F, Scarlata S and Agrò FE: COVID-19 diagnosis and management: A comprehensive review. *J Intern Med* 288: 192-206, 2020.
- Pelaia C, Tinello C, Vatrella A, De Sarro G and Pelaia G: Lung under attack by COVID-19-induced cytokine storm: Pathogenic mechanisms and therapeutic implications. *Ther Adv Respir Dis* 14: 1753466620933508, 2020.
- Fajgenbaum DC and June CH: Cytokine storm. *N Engl J Med* 383: 2255-2273, 2020.
- Mangalmurti N and Hunter CA: Cytokine storms: Understanding COVID-19. *Immunity* 53: 19-25, 2020.
- Fara A, Mitrev Z, Rosalia RA and Assas BM: Cytokine storm and COVID-19: A chronicle of pro-inflammatory cytokines. *Open Biol* 10: 200160, 2020.
- Ratajczak MZ, Bujko K, Ciechanowicz A, Sielatycka K, Cymer M, Marlicz W and Kucia M: SARS-CoV-2 entry receptor ACE2 is expressed on very small CD45⁺ precursors of hematopoietic and endothelial cells and in response to virus spike protein activates the Nlrp3 inflammasome. *Stem Cell Rev Rep* 17: 266-277, 2021.
- Soumagne T, Winiszewski H, Besch G, Mahr N, Senot T, Costa P, Grillet F, Behr J, Mouhat B, Mourey G, *et al*: Pulmonary embolism among critically ill patients with ARDS due to COVID-19. *Respir Med Res* 78: 100789, 2020.
- Grasselli G, Tonetti T, Protti A, Langer T, Girardis M, Bellani G, Laffey J, Carrafiello G, Carsana L, Rizzuto C, *et al*: Pathophysiology of COVID-19-associated acute respiratory distress syndrome: A multicentre prospective observational study. *Lancet Respir Med* 8: 1201-1208, 2020.
- Matthay MA, Leligdowicz A and Liu KD: Biological mechanisms of COVID-19 acute respiratory distress syndrome. *Am J Respir Crit Care Med* 202: 1489-1491, 2020.
- Nasonov E and Samsonov M: The role of interleukin 6 inhibitors in therapy of severe COVID-19. *Biomed Pharmacother* 131: 110698, 2020.
- Andreakos E, Papadaki M and Serhan CN: Dexamethasone, pro-resolving lipid mediators and resolution of inflammation in COVID-19. *Allergy* 76: 626-628, 2021.
- de Simone G and Mancusi C: Finding the right time for anti-inflammatory therapy in COVID-19. *Int J Infect Dis* 101: 247-248, 2020.

13. Khalifa SAM, Yosri N, El-Mallah MF, Ghonaim R, Guo Z, Musharraf SG, Du M, Khatib A, Xiao J, Saeed A, *et al.*: Screening for natural and derived bio-active compounds in preclinical and clinical studies: One of the frontlines of fighting the coronaviruses pandemic. *Phytomedicine* 85: 153311, 2021.
14. Matveeva T, Khafizova G and Sokornova S: In search of herbal anti-SARS-Cov2 compounds. *Front Plant Sci* 11: 589998, 2020.
15. Ohkubo S, Dalla Via L, Grancara S, Kanamori Y, García-Argáez AN, Canettieri G, Arcari P, Toninello A and Agostinelli E: The antioxidant, aged garlic extract, exerts cytotoxic effects on wild-type and multidrug-resistant human cancer cells by altering mitochondrial permeability. *Int J Oncol* 53: 1257-1268, 2018.
16. Lee J, Zhao N, Fu Z, Choi J, Lee HJ and Chung M: Effects of garlic intake on cancer: A systematic review of randomized clinical trials and cohort studies. *Nutr Res Pract* 15: 773-788, 2021.
17. Kodera Y, Ushijima M, Amano H, Suzuki JI and Matsutomo T: Chemical and biological properties of S-1-propenyl-L-cysteine in aged garlic extract. *Molecules* 22: 570, 2017.
18. Yeh YY and Liu L: Cholesterol-lowering effect of garlic extracts and organosulfur compounds: Human and animal studies. *J Nutr* 131 (3S): 989S-993S, 2001.
19. Nango H and Ohtani M: S-1-propenyl-L-cysteine suppresses lipopolysaccharide-induced expression of matrix metalloproteinase-1 through inhibition of tumor necrosis factor- α converting enzyme-epidermal growth factor receptor axis in human gingival fibroblasts. *PLoS One* 18: e0284713, 2023.
20. Ushijima M, Takashima M, Kunimura K, Kodera Y, Morihara N and Tamura K: Effects of S-1-propenylcysteine, a sulfur compound in aged garlic extract, on blood pressure and peripheral circulation in spontaneously hypertensive rats. *J Pharm Pharmacol* 70: 559-565, 2018.
21. Gasparello J, d'Aversa E, Breveglieri G, Borgatti M, Finotti A and Gambari R: In vitro induction of interleukin-8 by SARS-CoV-2 spike protein is inhibited in bronchial epithelial IB3-1 cells by a miR-93-5p agomiR. *Int Immunopharmacol* 101: 108201, 2021.
22. Zurlo M, Gasparello J, Verona M, Papi C, Cosenza LC, Finotti A, Marzaro G and Gambari R: The anti-SARS-CoV-2 BNT162b2 vaccine suppresses mithramycin-induced erythroid differentiation and expression of embryonic-fetal globin genes in human erythroleukemia K562 cells. *Exp Cell Res* 433: 113853, 2023.
23. Jiménez-Martín E, Ruiz J, Pérez-Palacios T, Silva A and Antequera T: Gas chromatography-mass spectrometry method for the determination of free amino acids as their dimethyl-tert-butylsilyl (TBDMS) derivatives in animal source food. *J Agric Food Chem* 60: 2456-2463, 2012.
24. Gasparello J, Lomazzi M, Papi C, D'Aversa E, Sansone F, Casnati A, Donofrio G, Gambari R and Finotti A: Efficient delivery of MicroRNA and AntimiRNA molecules using an argininovaline[4]arene macrocycle. *Mol Ther Nucleic Acids* 18: 748-763, 2019.
25. Aldén M, Olofsson Falla F, Yang D, Barghouth M, Luan C, Rasmussen M and De Marinis Y: Intracellular reverse transcription of pfizer BioNTech COVID-19 mRNA vaccine bnt162b2 in vitro in human liver cell line. *Curr Issues Mol Biol* 44: 1115-1126, 2022.
26. Livak KJ and Schmittgen TD: Analysis of relative gene expression data using real-time quantitative PCR and the 2(-Delta Delta C(T)) Method. *Methods* 25: 402-408, 2001.
27. Patra MC, Kwon HK, Batool M and Choi S: Computational insight into the structural organization of full-length Toll-like receptor 4 dimer in a model phospholipid bilayer. *Front Immunol* 9: 489, 2018.
28. Hanwell MD, Curtis DE, Lonie DC, Vandermeersch T, Zurek E and Hutchison GR: Avogadro: An advanced semantic chemical editor, visualization, and analysis platform. *J Cheminform* 4: 17, 2012.
29. Eberhardt J, Santos-Martins D, Tillack AF and Forli S: AutoDock Vina 1.2.0: New docking methods, expanded force field, and python bindings. *J Chem Inf Model* 61: 3891-3898, 2021.
30. Abraham MJ, Murtola T, Schulz R, Páll S, Smith JC, Hess B and Lindahl E: GROMACS: High performance molecular simulations through multi-level parallelism from laptops to supercomputers. *SoftwareX* 1-2: 19-25, 2015.
31. Bonomi M, Branduardi D, Bussi G, Camilloni C, Provasi D, Raiteri P, Donadio D, Marinelli F, Pietrucci F, Broglia RA and Parrinello M: PLUMED: A portable plugin for free-energy calculations with molecular dynamics. *Comput Phys Commun* 180: 1961-1972, 2009.
32. Huang J and MacKerell AD Jr: CHARMM36 all-atom additive protein force field: Validation based on comparison to NMR data. *J Comput Chem* 34: 2135-2145, 2013.
33. Darden T, York D and Pedersen L: Particle mesh Ewald: An N-log(N) method for Ewald sums in large systems. *J Chem Phys* 98: 10089-10092, 1993.
34. Hess B: P-LINCS: A parallel linear constraint solver for molecular simulation. *J Chem Theory Comput* 4: 116-122, 2008.
35. Evans D and Holian B: The nose-hoover thermostat. *J Chem Phys* 83: 4069-4074, 1985.
36. Parrinello M and Rahman A: Polymorphic transitions in single crystals: A new molecular dynamics method. *J Appl Phys* 52: 7182-7190, 1981.
37. Tupini C, Zurlo M, Gasparello J, Lodi I, Finotti A, Scattolin T, Visentin F, Gambari R and Lampronti I: Combined treatment of cancer cells using allyl palladium complexes bearing purine-based NHC ligands and molecules targeting MicroRNAs miR-221-3p and miR-222-3p: Synergistic effects on apoptosis. *Pharmaceutics* 15: 1332, 2023.
38. Cari L, Naghavi Alhosseini M, Mencacci A, Migliorati G and Nocentini G: Differences in the expression levels of SARS-CoV-2 spike protein in cells treated with mRNA-based COVID-19 vaccines: A study on vaccines from the real world. *Vaccines (Basel)* 11: 879, 2023.
39. Bansal S, Perincheri S, Fleming T, Poulson C, Tiffany B, Bremner RM and Mohanakumar T: Cutting edge: Circulating exosomes with COVID spike protein are induced by BNT162b2 (Pfizer-BioNTech) Vaccination prior to Development of Antibodies: A novel mechanism for immune activation by mRNA vaccines. *J Immunol* 207: 2405-2410, 2021.
40. Gambari R, Papi C, Gasparello J, Agostinelli E and Finotti A: Preliminary results and a theoretical perspective of co-treatment using a miR-93-5p mimic and aged garlic extract to inhibit the expression of the pro-inflammatory interleukin-8 gene. *Exp Ther Med* 29: 85, 2025.
41. Kodera Y, Matsutomo T and Itoh K: The evidence for the production mechanism of cis-S-1-propenylcysteine in aged garlic extract based on a model reaction approach using its isomers and deuterated solvents. *Planta Med Lett* 2: e69-e72, 2015.
42. Kircheis R and Planz O: Could a lower Toll-like receptor (TLR) and NF- κ B activation due to a changed charge distribution in the spike protein be the reason for the lower pathogenicity of omicron? *Int J Mol Sci* 23: 5966, 2022.
43. Robles JP, Zamora M, Adán-Castro E, Siqueiros-Marquez L, Martínez de la Escalera G and Clapp C: The spike protein of SARS-CoV-2 induces endothelial inflammation through integrin α 5 β 1 and NF- κ B signaling. *J Biol Chem* 298: 101695, 2022.
44. Forsyth CB, Zhang L, Bhushan A, Swanson B, Zhang L, Mamede JI, Voigt RM, Shaikh M, Engen PA and Keshavarzian A: The SARS-CoV-2 S1 spike protein promotes MAPK and NF- κ B activation in human lung cells and inflammatory cytokine production in human lung and intestinal epithelial cells. *Microorganisms* 10: 1996, 2022.
45. Gasparello J, D'Aversa E, Papi C, Gambari L, Grigolo B, Borgatti M, Finotti A and Gambari R: Sulforaphane inhibits the expression of interleukin-6 and interleukin-8 induced in bronchial epithelial IB3-1 cells by exposure to the SARS-CoV-2 spike protein. *Phytomedicine* 87: 153583, 2021.
46. Múnera-Rodríguez AM, Leiva-Castro C, Sobrino F, López-Enríquez S and Palomares F: Sulforaphane-mediated immune regulation through inhibition of NF- κ B and MAPK signaling pathways in human dendritic cells. *Biomed Pharmacother* 177: 117056, 2024.
47. Gasparello J, Marzaro G, Papi C, Gentili V, Rizzo R, Zurlo M, Scapoli C, Finotti A and Gambari R: Effects of sulforaphane on SARS-CoV-2 infection and NF- κ B dependent expression of genes involved in the COVID-19 'cytokine storm'. *Int J Mol Med* 52: 76, 2023.
48. Dharrar R, Kumar Sharma A and Datta S: Emerging aspects of cytokine storm in COVID-19: The role of proinflammatory cytokines and therapeutic prospects. *Cytokine* 169: 156287, 2023.
49. Leavis HL, van de Veerendonk FL and Murthy S: Stimulating severe COVID-19: The potential role of GM-CSF antagonism. *Lancet Respir Med* 10: 223-224, 2022.
50. Cherubini A, Rusconi F and Lazzari L: Identification of the best housekeeping gene for RT-qPCR analysis of human pancreatic organoids. *PLoS One* 16: e0260902, 2021.

51. Gentile AM, Lhamyani S, Coín-Aragüez L, Oliva-Olivera W, Zayed H, Vega-Rioja A, Monteseirin J, Romero-Zerbo SY, Tinahones FJ, Bermúdez-Silva FJ and El Bekay R: RPL13A and EEF1A1 are suitable reference genes for qPCR during adipocyte differentiation of vascular stromal cells from patients with different BMI and HOMA-IR. *PLoS One* 11: e0157002, 2016.
52. Pease JE and Sabroe I: The role of interleukin-8 and its receptors in inflammatory lung disease: Implications for therapy. *Am J Respir Med* 1: 19-25, 2002.
53. Molnar V, Matišić V, Kodvanj I, Bjelica R, Jeleč Ž, Hudetz D, Rod E, Čukelj F, Vrdoljak T, Vidović D, *et al*: Cytokines and chemokines involved in osteoarthritis pathogenesis. *Int J Mol Sci* 22: 9208, 2021.
54. Marzaro G, Lampronti I, D'Aversa E, Sacchetti G, Miolo G, Vaccarin C, Cabrini G, Dechecchi MC, Gambari R and Chilin A: Design, synthesis and biological evaluation of novel trimethyl-angelicin analogues targeting nuclear factor κB (NF-κB). *Eur J Med Chem* 151: 285-293, 2018.
55. Gambari R, Borgatti M, Lampronti I, Fabbri E, Brognara E, Bianchi N, Piccagli L, Yuen MCW, Kan CW, Hau DKP, *et al*: Corilagin is a potent inhibitor of NF-kappaB activity and down-regulates TNF-alpha induced expression of IL-8 gene in cystic fibrosis IB3-1 cells. *Int Immunopharmacol* 13: 308-315, 2012.
56. Doyle SL and O'Neill LAJ: Toll-like receptors: From the discovery of NFκappaB to new insights into transcriptional regulations in innate immunity. *Biochem Pharmacol* 72: 1102-1113, 2006.
57. Carmody RJ and Chen YH: Nuclear factor-kappaB: Activation and regulation during Toll-like receptor signaling. *Cell Mol Immunol* 4: 31-41, 2007.
58. Verstrepen L, Bekaert T, Chau TL, Tavernier J, Chariot A and Beyaert R: TLR-4, IL-1R and TNF-R signaling to NF-kappaB: Variations on a common theme. *Cell Mol Life Sci* 65: 2964-2978, 2008.
59. Zeng Z, Yu H, Chen H, Qi W, Chen L, Chen G, Yan W, Chen T, Ning Q, Han M and Wu D: Longitudinal changes of inflammatory parameters and their correlation with disease severity and outcomes in patients with COVID-19 from Wuhan, China. *Crit Care* 24: 525, 2020.
60. Del Valle DM, Kim-Schulze S, Huang HH, Beckmann ND, Nirenberg S, Wang B, Lavin Y, Swartz TH, Madduri D, Stock A, *et al*: An inflammatory cytokine signature predicts COVID-19 severity and survival. *Nat Med* 26: 1636-1643, 2020.
61. Burke H, Freeman A, Cellura DC, Stuart BL, Brendish NJ, Poole S, Borca F, Phan HTT, Sheard N, Williams S, *et al*: Inflammatory phenotyping predicts clinical outcome in COVID-19. *Respir Res* 21: 245, 2020.
62. Aldallal N, McNaughton EE, Manzel LJ, Richards AM, Zabner J, Ferkol TW and Look DC: Inflammatory response in airway epithelial cells isolated from patients with cystic fibrosis. *Am J Respir Crit Care Med* 166: 1248-1256, 2002.
63. Maiuri L, Luciani A, Giardino I, Raia V, Villella VR, D'Apolito M, Pettoello-Lucantoni M, Guido S, Ciacci C, Cimmino M, *et al*: Tissue transglutaminase activation modulates inflammation in cystic fibrosis via PPARγ down-regulation. *J Immunol* 180: 7697-7705, 2008.
64. Bhattacharyya S, Balakathiresan NS, Dalgard C, Gutti U, Armistead D, Jozwik C, Srivastava M, Pollard HB and Biswas R: Elevated miR-155 promotes inflammation in cystic fibrosis by driving hyperexpression of interleukin-8. *J Biol Chem* 286: 11604-11615, 2011.
65. Balakathiresan NS, Bhattacharyya S, Gutti U, Long RP, Jozwik C, Huang W, Srivastava M, Pollard HB and Biswas R: Tristetraprolin regulates IL-8 mRNA stability in cystic fibrosis lung epithelial cells. *Am J Physiol Lung Cell Mol Physiol* 296: L1012-L1018, 2009.
66. Kanamori Y, Via LD, Macone A, Canettieri G, Greco A, Toninello A and Agostinelli E: Aged garlic extract and its constituent, S-allyl-L-cysteine, induce the apoptosis of neuroblastoma cancer cells due to mitochondrial membrane depolarization. *Exp Ther Med* 19: 1511-1521, 2020.
67. Amano H, Kazamori D and Itoh K: Pharmacokinetics and N-acetylation metabolism of S-methyl-L-cysteine and trans-S-1-propenyl-L-cysteine in rats and dogs. *Xenobiotica* 46: 1017-1025, 2016.
68. Amano H, Kazamori D and Itoh K: Evaluation of the effects of S-allyl-L-cysteine, S-methyl-L-cysteine, trans-S-1-propenyl-L-cysteine, and their N-acetylated and S-oxidized metabolites on human CYP activities. *Biol Pharm Bull* 39: 1701-1707, 2016.
69. Soy M, Keser G, Atagündüz P, Tabak F, Atagündüz I and Kayhan S: Cytokine storm in COVID-19: Pathogenesis and overview of anti-inflammatory agents used in treatment. *Clin Rheumatol* 39: 2085-2094, 2020.
70. Mustafa MI, Abdelmoneim AH, Mahmoud EM and Makhawi AM: Cytokine storm in COVID-19 patients, its impact on organs and potential treatment by QTY code-designed detergent-free chemokine receptors. *Mediators Inflamm* 2020: 8198963, 2020.
71. Gasparello J, Papi C, Marzaro G, Macone A, Zurlo M, Finotti A, Agostinelli E and Gambari R: Aged garlic extract (AGE) and its constituent S-allyl-cysteine (SAC) inhibit the expression of pro-inflammatory genes induced in bronchial epithelial IB3-1 cells by exposure to the SARS-CoV-2 spike protein and the BNT162b2 vaccine. *Molecules* 29: 5938, 2024.
72. Choudhury A and Mukherjee S: In silico studies on the comparative characterization of the interactions of SARS-CoV-2 spike glycoprotein with ACE-2 receptor homologs and human TLRs. *J Med Virol* 92: 2105-2113, 2020.
73. Shirato K and Kizaki T: SARS-CoV-2 spike protein S1 subunit induces pro-inflammatory responses via Toll-like receptor 4 signaling in murine and human macrophages. *Heliyon* 7: e06187, 2021.
74. Zhao Y, Kuang M, Li J, Zhu L, Jia Z, Guo X, Hu Y, Kong J, Yin H, Wang X and You F: SARS-CoV-2 spike protein interacts with and activates TLR4. *Cell Res* 31: 818-820, 2021.
75. Chakraborty C, Mallick B, Bhattacharya M and Byrareddy SN: SARS-CoV-2 omicron spike shows strong binding affinity and favourable interaction landscape with the TLR4/MD2 compared to other variants. *J Genet Eng Biotechnol* 22: 100347, 2024.
76. Aboudounya MM and Heads RJ: COVID-19 and Toll-Like Receptor 4 (TLR4): SARS-CoV-2 may bind and activate TLR4 to increase ACE2 expression, facilitating entry and causing hyperinflammation. *Mediators Inflamm* 2021: 8874339, 2021.
77. Kawai T and Akira S: Signaling to NF-kappaB by Toll-like receptors. *Trends Mol Med* 13: 460-469, 2007.
78. Tang S, Liang Y, Wang M, Lei J, Peng Y, Tao Q, Ming T, Yang W, Zhang C, Guo J and Xu H: Qinhuo Shanggan oral solution resolves acute lung injury by down-regulating TLR4/NF-κB signaling cascade and inhibiting NLRP3 inflammasome activation. *Front Immunol* 14: 1285550, 2023.
79. Kaushik D, Bhandari R and Kuhad A: TLR4 as a therapeutic target for respiratory and neurological complications of SARS-CoV-2. *Expert Opin Ther Targets* 25: 491-508, 2021.
80. Yang G, Zhang S, Wang Y, Li L, Li Y, Yuan D, Luo F, Zhao J, Song X and Zhao Y: Aptamer blocking S-TLR4 interaction selectively inhibits SARS-CoV-2 induced inflammation. *Signal Transduct Target Ther* 7: 120, 2022.
81. Asaba CN, Ekabe CJ, Ayuk HS, Gwanyama BN, Bitazar R and Bukong TN: Interplay of TLR4 and SARS-CoV-2: Unveiling the complex mechanisms of inflammation and severity in COVID-19 infections. *J Inflamm Res* 17: 5077-5091, 2024.
82. Verbeke R, Hogan MJ, Loré K and Pardi N: Innate immune mechanisms of mRNA vaccines. *Immunity* 55: 1993-2005, 2022.
83. Sartorius R, Trovato M, Manco R, D'Apice L and De Berardinis P: Exploiting viral sensing mediated by Toll-like receptors to design innovative vaccines. *NPJ Vaccines* 6: 127, 2021.
84. Delehedde C, Even L, Midoux P, Pichon C and Perche F: Intracellular routing and recognition of lipid-based mRNA nanoparticles. *Pharmaceutics* 13: 945, 2021.
85. Da Costa CBP, Cruz ACM, Penha JCQ, Castro HC, Da Cunha LER, Ratcliffe NA, Cisne R and Martins FJ: Using in vivo animal models for studying SARS-CoV-2. *Expert Opin Drug Discov* 17: 121-137, 2022.
86. Wlosinska M, Nilsson AC, Hlebowicz J, Fakhro M, Malmsjö M and Lindstedt S: Aged garlic extract reduces IL-6: A double-blind placebo-controlled trial in females with a low risk of cardiovascular disease. *Evid Based Complement Alternat Med* 2021: 6636875, 2021.
87. Xu C, Mathews AE, Rodrigues C, Eudy BJ, Rowe CA, O'Donoghue A and Percival SS: Aged garlic extract supplementation modifies inflammation and immunity of adults with obesity: A randomized, double-blind, placebo-controlled clinical trial. *Clin Nutr ESPEN* 24: 148-155, 2018.
88. Fabbri E, Borgatti M, Montagner G, Bianchi N, Finotti A, Lampronti I, Bezzetti V, Dechecchi MC, Cabrini G and Gambari R: Expression of microRNA-93 and interleukin-8 during *Pseudomonas aeruginosa*-mediated induction of proinflammatory responses. *Am J Respir Cell Mol Biol* 50: 1144-1155, 2014.

89. De Stefano D, Ungaro F, Giovino C, Polimeno A, Quaglia F and Carnuccio R: Sustained inhibition of IL-6 and IL-8 expression by decoy ODN to NF- κ B delivered through respirable large porous particles in LPS-stimulated cystic fibrosis bronchial cells. *J Gene Med* 13: 200-208, 2011.
90. Lampronti I, Dehecchi MC, Rimessi A, Bezzeri V, Nicolis E, Guerrini A, Tacchini M, Tamanini A, Munari S, D'Aversa E, *et al*: β -Sitosterol reduces the expression of chemotactic cytokine genes in cystic fibrosis bronchial epithelial cells. *Front Pharmacol* 8: 236, 2017.
91. Hawdon NA, Aval PS, Barnes RJ, Gravelle SK, Rosengren J, Khan S, Ciofu O, Johansen HK, Høiby N and Ulanova M: Cellular responses of A549 alveolar epithelial cells to serially collected *Pseudomonas aeruginosa* from cystic fibrosis patients at different stages of pulmonary infection. *FEMS Immunol Med Microbiol* 59: 207-220, 2010.
92. Demonbreun AR, Velez MP, Saber R, Ryan DT, Sancilio A, McDade TW and McNally EM: mRNA intramuscular vaccination produces a robust IgG antibody response in advanced neuromuscular disease. *Neuromuscul Disord* 32: 33-35, 2022.
93. Elmazoglu Z, Aydın Bek Z, Sarıbaş SG, Özoğul C, Goker B, Bitik B, Aktekin CN and Karasu Ç: S-allylcysteine inhibits chondrocyte inflammation to reduce human osteoarthritis via targeting RAGE, TLR4, JNK, and Nrf2 signaling: Comparison with colchicine. *Biochem Cell Biol* 99: 645-654, 2021.
94. Shao Z, Pan Z, Lin J, Zhao Q, Wang Y, Ni L, Feng S, Tian N, Wu Y, Sun L, *et al*: S-allyl cysteine reduces osteoarthritis pathology in the tert-butyl hydroperoxide-treated chondrocytes and the destabilization of the medial meniscus model mice via the Nrf2 signaling pathway. *Aging (Albany NY)* 12: 19254-19272, 2020.
95. Cantin AM, Hartl D, Konstan MW and Chmiel JF: Inflammation in cystic fibrosis lung disease: Pathogenesis and therapy. *J Cyst Fibros* 14: 419-430, 2015.
96. Lemanske RF Jr: Inflammatory events in asthma: An expanding equation. *J Allergy Clin Immunol* 105: S633-S636, 2000.
97. Xu J, Zeng Q, Li S, Su Q and Fan H: Inflammation mechanism and research progress of COPD. *Front Immunol* 15: 1404615, 2024.
98. Degan D, Ornello R, Tiseo C, Carolei A, Sacco S and Pistoia F: The role of inflammation in neurological disorders. *Curr Pharm Des* 24: 1485-1501, 2018.
99. Ji Y, Li M, Chang M, Liu R, Qiu J, Wang K, Deng C, Shen Y, Zhu J, Wang W, *et al*: Inflammation: Roles in skeletal muscle atrophy. *Antioxidants (Basel)* 11: 1686, 2022.
100. Hencin MY, Vancheri S, Longo G and Vancheri F: The role of inflammation in cardiovascular disease. *Int J Mol Sci* 23: 12906, 2022.
101. Tsalamandris S, Antonopoulos AS, Oikonomou E, Papamikroulis GA, Vogiatzi G, Papaioannou S, DeFtereos S and Tousoulis D: The role of inflammation in diabetes: Current concepts and future perspectives. *Eur Cardiol* 14: 50-59, 2019.
102. Coussens LM and Werb Z: Inflammation and cancer. *Nature* 420: 860-867, 2002.
103. Zhao H, Wu L, Yan G, Chen Y, Zhou M, Wu Y and Li Y: Inflammation and tumor progression: Signaling pathways and targeted intervention. *Signal Transduct Target Ther* 6: 263, 2021.



Copyright © 2025 Papi et al. This work is licensed under a Creative Commons Attribution-NonCommercial-NoDerivatives 4.0 International (CC BY-NC-ND 4.0) License.